European Review for Medical and Pharmacological Sciences 2023; 27: 10112-10125

Green synthesized silver nanoparticles using the plant-based reducing agent *Matricaria chamomilla* induce cell death in colorectal cancer cells

A.A.H. ABDELLATIF[1,2], H.A. MOHAMMED[3,4], M.H. ABDULLA[5], A.M. ALSUBAIYEL[1], A. MAHMOOD[6], W.A. SAMMAN[7], A.A. ALHADDAD[7], O. AL RUGAIE[8], M. ALSHARIDAH[9], M.A. VAALI-MOHAMMED[5], N. AL HASSAN[5], H.H. TAHA[10]

[1]Department of Pharmaceutics, College of Pharmacy, Qassim University, Qassim, Saudi Arabia
[2]Department of Pharmaceutics and Pharmaceutical Technology, Faculty of Pharmacy, Al-Azhar University, Assiut, Egypt
[3]Department of Medicinal Chemistry and Pharmacognosy, College of Pharmacy, Qassim University, Buraidah, Saudi Arabia
[4]Department of Pharmacognosy, Faculty of Pharmacy, Al-Azhar University, Cairo, Egypt
[5]Department of Surgery, King Saud University, College of Medicine, Colorectal Research Chair, Riyadh, Saudi Arabia
[6]Department of Anatomy, Stem Cell Unit, College of Medicine, King Saud University, Riyadh, Saudi Arabia
[7]Department of Pharmacology and Toxicology, College of Pharmacy College, Taibah University, Medina, Saudi Arabia
[8]Department of Basic Medical Sciences, College of Medicine and Medical Sciences, Qassim University, Unaizah, Saudi Arabia
[9]Department of Physiology, College of Medicine, Qassim University, Buraydah, Saudi Arabia
[10]Department of Biochemistry, Faculty of Pharmacy, Al-Azhar University, Assiut, Egypt

Abstract. – OBJECTIVE: There is a need to treat cancer cells with safe and natural nanoparticles to avoid the side effects of chemotherapeutic agents. Chamomile is considered a safe, natural plant with anticancer activity. We synthesize simple, inexpensive, and eco-friendly silver nanoparticles (SNs) using Chamomile (CHM) to tune their anticancer properties.

MATERIALS AND METHODS: SN-CHM was synthesized by reducing 1 mM silver nitrate aqueous solution in 100 mL with the aqueous ethanolic flower extract of CHM (18 mg/mL, w/v). The reaction proceeded overnight at 600 rpm and 28°C. SN-CHM was characterized for their % yield, average diameter, charge, morphology, and silver release. Moreover, SN-CHM was investigated for its antioxidant and anticancer activities at 200 µg/mL and 5 mg/ mL, respectively.

RESULTS: A 59.12% yield and a uniform SN-CHM size of 115 ± 3.1 nm with a ζ-potential of -27.67 ± (-3.92) mv were observed. The UV-visible absorption showed shifts from 379.5 to 383.5 nm for CHM and SN-CHM, respectively. Moreover, Ag^+ was ultimately released from SN-CHM after 5 h. Fourier Transform Infrared Spectroscopy (FT-IR) showed characteristic absorption peaks of CHM and produced SN-CHM. Furthermore, SN-CHM showed moderate antioxidant activity. SN-CHM inhibited the % viability of SW620 and HT-29 cell lines at 20 µM. SN-CHM may also greatly upregulate the apoptotic gene BAX while considerably downregulating the anti-apoptotic genes BCL2 and BCL-XI.

CONCLUSIONS: CHM can be a safe soft drink, especially when conjugated with Ag ions as anticancer NPs. SN-CHM is considered potent anticancer activity against SW620, and HT-29 cell lines.

Key Words:
Anticancer activities, Nanoparticle, Silver, *Matricaria chamomilla.*

Introduction

Using non-toxic and environmentally acceptable compounds as reducing agents has recently gained popularity due to the need for using silver nanoparticles (SN) in biomedical applications and sustainable development[1]. Natural compounds and eco-friendliness, such as apple extract, synthesize SN for antibacterial properties[2]. Saffron

Corresponding Author: Ahmed A.H. Abdellatif, MD; e-mail: a.abdellatif@qu.edu.sa

extract was also employed to deliver SN for antimicrobial purposes[3]. Green and environmentally friendly synthesis is also being investigated for relatively high applications[1].

In this study, we used Chamomile (CHM), *Matricaria chamomilla L.*, or German Chamomile as a source of reduction to produce SN in an environmentally safe[4,5]. CHM is a globally famous plant used in traditional medicine to treat anxiety and gastrointestinal (GIT) disorders. CHM is commercially available as an herbal tea for treating infant GIT cramps. Biologically, CHM was shown to be anti-inflammatory, antioxidant, anticancer, and neuroprotective. Furthermore, it has growth-inhibitory effects on cancer and ovarian tumor models[6]. Additionally, CHM was shown to induce apoptosis in cancer cells[7]. Therefore, we focused our study on the anticancer activities of SN reduced with CHM, especially on GIT cancers.

SNs have a wide variety of uses in medical devices, medicines, textiles, and water purification, as well as in the adsorption of metals and pesticides, sensing of food contaminants, and DNA detection[8]. SN can be used mainly in diagnosing and treating cancer due to the unique optical and localized surface plasmon resonance (LSPR) and lower cytotoxicity of Ag[9]. CHM was used in the green synthesis of SN-CHM to reduce Ag^+ to Ag^0 and formulate eco-friendly and less toxic silver nanoparticles[10].

CHM is an aromatic plant rich in volatile constituents, e.g., chamazulene and α-terpineol. However, the main volatile constituent of Chamomile is the essential oil terpenoid α-bisabolol[11]. In addition, flavonoids and phenolic acids such as caffeic acid, luteolin, luteolin-7-*O*-glucoside apigenin, and apigenin-7-*O*-glucoside were detected in the polar extracts of Chamomile[12]. Therefore, a focus on drug production of potentially powerful and effective anticancer treatments is strongly urged among the different drug discovery methods. Natural products have proven effective at revealing new leads and unique candidates[13]. The plant extract used is highly advantageous because it is fast, safer, less risky, and less biodegradable than the standard nonliving synthesis processes[14]. This study aimed to synthesize SN using aqueous extracts of CHM, whose bulb is a rich source of the terpenoid α-bisabolol. The produced SN-CHMs were characterized for their morphology, release, Fourier Transform Infrared Spectroscopy (FT-IR), and SEM. SN-CHM was tested against cancer cell lines to prove its enhanced anticancer and antioxidant potential activities.

Materials and Methods

Chamomile (CHM) was obtained from the Saudi market (Buraydah, Al Qassim, Saudi Arabia). It was classified as *Matricaria chamomilla L.* by specialists and taxonomists (Department of Plant Production and Protection, Qassim University). HCl, HNO_3, and $AgNO_3$ were purchased from GLOBAL CHEMIE (Vadodara, India). Ammonium molybdate and ascorbic acid were purchased from (Sarkhej, Ahmedabad, Gujarat, India). Total antioxidant capacity (TAC), 2,2-diphenyl-1-picrylhydrazyl (DPPH), ferric reducing antioxidant power (FRAP), (4,5-dimethylthiazol-2-yl)-2,5-diphenyltetrazolium bromide) (MTT), and dimethylsulfoxide (DMSO) were obtained from Sigma Aldrich (St. Louis, MO, USA). From ATCC, we purchased human colorectal cancer cell lines (SW620 and HT-29 cells) (Manassas, VA, USA). All cultures were grown at 37°C in a humid environment with 5% CO_2. Every chemical was of analytical grade. Using Millipore water, all glassware was washed.

Plant Material and Extraction Procedure

Chamomile aerial parts were dried at 50°C in the oven for 3 continuous days to remove moisture. At a temperature of 50°C, the CHM's maximum humidity was held at a relative moisture percent of 20% for all drying air temperatures[15]. The plant was then ground to a fine powdered form. Exactly 1 g of the plant powder was extracted using an aqueous ethanol mixture (100 mL of distilled water: ethanol, 70:30). The extract was stirred for 24 h using a magnetic stirrer and filtered through Whatman filter paper.

Preparation of SN-CHM

SN-CHM was prepared as previously described with minor modifications[16,17]. Concisely, 33.96 mg ≅ (2 mM) silver nitrate ($AgNO_3$) was prepared and stirred with aqueous extracted CHM using a multiple stirrer (VELP-Scientifica-Srl, Italy). The stirring proceeded at 28 ± 2°C. SN-CHM was fabricated by detecting a color change from yellowish to wine-red. The obtained SN-CHMs were stored in a dark place away from light (Figure 1).

Characterization of SN

The percentage yield of synthesized SN

The amount of Ag^+ converted to Ag^0 denotes the % yield of the produced SN-CHM depending on the previously reported procedure with minor adjustments[18]. The amount of Ag^0 in SN-CHM was determined using inductively coupled pla-

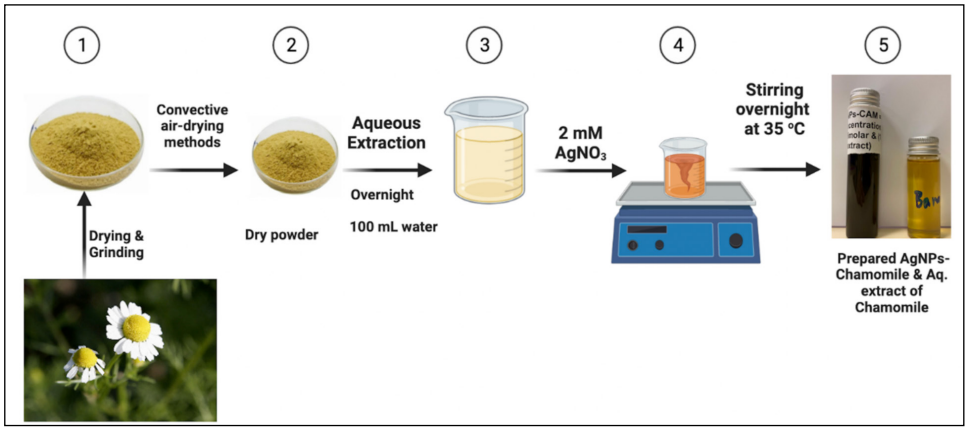

Figure 1. Schematic diagram for the preparation of SNs-CHM.

sma-optical emission spectrometry (ICP-OES) (iCAP 6000, Thermo Scientific, Waltham, MA, USA). The blank sample was 5% HNO_3/H_2O for detecting free Ag^+ at 324 nm. The samples were diluted 20 times with 5% HNO_3 and tested for total Ag^0 (SN-CHM plus unreacted Ag^+). Then, the same concentration of NaCl as $AgNO_3$ was added to each sample test to precipitate Ag^+ as AgCl. After 12 h, the AgCl was centrifuged for 13 min at 2,000 rpm and analyzed using ICP-OES. The total Ag^0 in the reduced SN-CHM was then determined from the supernatant SN. Each solution was scanned 5 times. The % yield of Ag^0 can be calculated by dividing the obtained concentration by the initial concentration of $AgNO_3$ using the equation:

Eq. 1.

$$\%\ \mathrm{SN-CHM\ yield} = \left[\frac{Concentration\ of\ sample\ by\ ICP-OES}{Initial\ Concentration\ of\ AgNO3}\right] x\ 100$$

Size and Charge

A Malvern Zetasizer Nano, manufactured by Malvern Instruments GmbH (Herrenberg, Germany), was used to measure the size and charge of the synthesized SN-CHM with compliant software as an option and sample measurements at many concentrations without diluting or concentrating. SN-CHM was adjusted to 25°C and put through a laser beam of 623 nm[9,19].

SEM Analysis

The morphology of the produced nanoparticles was examined using scanning electron microscopy (Carl Zeiss, Germany). Before imaging in SEM equipment, the SN-CHM was coated with a thin layer of platinum using a coating unit (Sputter coater, JOEL JFC-1300) in a vacuum for 55 sec at 25 mÅ[20].

Ultraviolet-Visible Spectroscopy

The CHM extract and SN-CHM were examined using UV-Vis (Jasco, UV-630, Japan) spectrophotometry for the maximum wavelength and shift[21,22].

Fourier Transform Infrared Spectroscopy (FT-IR)

An FT-IR spectrometer (Thermo SCIENTIFIC Co., Twin, USA) 9 was used to analyze the compatibility of CHM and CHM-associated SN formation. Therefore, our aim here was to prove the formation of SN-CHM, and absorption peaks were detected at 400-4,000 cm^{-1}.

Silver Ion Release

The release of Ag^0 from the prepared SN-CHM was achieved as previously described with minor modifications[23]. A thin film layer was prepared (≅ 3 cm^2) and subjected to release by incubating SN-CHM in 50 mL deionized water for 24 h. After careful calibration with standard Ag solution, samples were taken at different time intervals for Ag^0 measurement. The experiment proceeded in triplicate at room temperature (25°C) using an orbital shaker (WiseShak, SHO-2D, Korea) at 100 rpm.

Antioxidant Activity Screening

Three in vitro assays were conducted to measure the antioxidant activity of the CHM extract and the formulated SN-CHM. The results were expressed as mg Trolox equivalents using calibration curves. All the methods were repeated three times, and the mean and standard deviations were calculated.

Total Antioxidant Capacity (TAC)

The reducing ability of CHM and SN-CHM to molybdate ions was determined using the literature method[24], in which 200 µl containing 200 µg of the samples (CHM or SN-CHM) was mixed

with 2 mL of molybdate reagent. The mixture was incubated in a warm water bath for 30 min. The developed blue color was measured at 695 nm.

Ferric Reducing Antioxidant Power (FRAP) Method

Freshly FRAP reagent was prepared using CHM and SN-CHM to reduce ferric ions[24]. The FRAP and the nanoparticle reaction mixture were prepared: 2 mL of the reagent and 0.1 mL of CHM or SN-CHM (200 µg) were mixed and incubated for 30 min before measuring the absorbance at 593 nm[25].

DPPH Scavenging Activity

The reduction in the DPPH radical color indicates the ability of products to scavenge free radicals[26]. The ability of CHM and SN-CHM to reduce the DPPH color was assessed as mentioned in the literature[27] with modifications. To the DPPH (300 M) solution, equal volumes of CHM or SN-CHM solution were added. After 30 min of incubation, the reduction in the violet color was measured at 517 nm.

Cell Culture

The human adenocarcinoma colorectal cancer cell line HT-29 and metastatic colorectal cancer cell line SW620 were purchased from ATCC (Manassas, VA, USA). HT-29 cells and SW620 cells were maintained in RPMI-1640 media (10% heat-inactivated fetal bovine serum) (Thermo Fisher Scientific Inc, Waltham, MA, USA), 100 Unit/mL penicillin (Thermo Fisher Scientific Inc. Waltham, MA, USA), and 2 mM L-glutamine (Thermo Fisher Scientific Inc, Waltham, MA, USA). STR analysis was performed to confirm the new batches of cells. Testing for mycoplasma was performed on all cell lines. All cells were incubated at 37.2°C in a humidified atmosphere and 5% CO_2.

Cell Proliferation Assay

Cell proliferation was performed using 3-(4,5-dimethylthiazolyl-2)-2,5-diphenyltetrazolium bromide (MTT)[28,29] for SN-CHM and CHM extract against HT-29 and SW620 cancer cell lines. 1×10^6 cells/mL were seeded in 96 flat-bottom well plates. CHM, $AgNO_3$, and SN-CHM (5 mg/mL) were mixed with sterile distilled water and diluted to the required concentrations (50, 100, 150, 200, and 250 µg/mL). Appropriate concentrations of CHM, $AgNO_3$, and SN-CHM (50-250 µg/mL) were added to the cultures and incubated for 24 h in a 5% CO_2 atmosphere. Freshly prepared MTT solution (5 mM, 10 µL) was added to the cells and further incubated for 2 h at 37°C in 5% CO_2. DMSO was added to solubilize the formazan crystals. Utilizing a microplate reader, the optical density was measured at 540 nm for three separate experiments. The means and standard deviations (mean±SD) were calculated, and Eq. 1 was used to calculate the % growth inhibition.

$$\% \text{ growth inhibition} = \frac{(\text{A570 of treated cells})}{(\text{A570 of control cells})} \times 100 \quad \text{eq 1}$$

Quantitative Real-Time PCR (qRT-PCR)

Total RNA was extracted using a PureLink kit (Ambion by Life Technologies, USA, Cat No.: 12183018A) as suggested by the company. Total RNA was estimated by a Nanodrop spectrophotometer (Nanodrop-2000, Thermo Scientific, USA). Complementary DNA (cDNA) was produced from 1 µg of the RNA using a High-Capacity cDNA Reverse Transcription kit (Applied-Biosystem, USA) using a Labnet Multigene thermocycler according to the manufacturer's instructions. Relative levels of mRNA were determined from cDNA by real-time PCR (Applied Biosystem-Real Time PCR Detection System) with a Power SYBR Green PCR kit (Applied Biosystem, UK) or with TaqMan Universal Master Mix II, no UNG (Applied Biosystem, USA) according to the manufacturer's instructions. Following normalization to the reference gene *GAPDH*, quantification of gene expression was carried out using a comparative Ct method where ΔCT is the difference between the CT values of the target and reference gene.

Statistical Analysis

Each experiment was carried out in triplicate to determine statistical means and standard errors. Data analyses were performed using Statistical Package of Social Science (SPSS) Software version 25 (IBM Corp., Armonk, NY, USA). Two-way ANOVA was used to assess the statistical significance of differences in values between the treated and untreated (control) groups, and differences with $p < 0.05$ were deemed significant.

Results

The aqueous extracts of the CHM were used to reduce $AgNO_3$, causing the color to change from yellow to wine-red. This coloration indicated the formation of nanosilver SN-CHM. Differential light scattering (DLS) revealed uniform SN-CHM

with only one symmetrical peak of size 115 ± 3.1 nm (Figure 2A). The ζ-potentials recorded by DLS of SN-CHM were negative surface charges of -27.3 ± 3.92 mv. All recorded polydispersity indices (PDIs) were optimal and below 0.152, demonstrating a stable colloidal system (Figure 2A). Furthermore, SEM showed oval-shaped SN-CHM with a size range of 1 µm (Figure 2B).

The UV-visible absorption shifted from 378.5 to 388 nm for CHM and SN-CHM, respectively (Figure 3A). As CHM reduced $AgNO_3$ to SN-CHM, a color change was observed. SN-CHM has free electrons that generate the SPR band's resonance[30].

The functional groups of $AgNO_3$, CHM, and SN-CHM were checked by FT-IR (Figure 3B). The FT-IR also showed the typical peaks of CHM and $AgNO_3$ compared with SN-CHM. The bands at 3,410.00 and 3,370.0 cm^{-1} are related to the O-H stretching of phenol. The peaks (2,921.0 and 2,852.0 cm^{-1}) are representative of the C-H vibration (stretching) of glucosides. The bands (1,750.00 and 1,620.00 cm^{-1}) match the C=O vibration of bonded, coupled esters from luteolin[31]. The wide-ranging band centered throughout 1,050.00 cm^{-1} is recognized to be aromatic ethers and polysaccharides (C-O-C stretching). The bands (900-600 cm^{-1}) match the amines and amides of CHM. The FT-IR spectrum of SN-CHM does not include the band at 1,109.00 cm^{-1}, which resembles the C-O groups of polyols such as flavones, terpenoids, and polysaccharides. These confirmed polyols are responsible for reducing silver ions, producing FT-IR spectra with two main groups of peaks[10].

The Ag^+ was released continually in an aqueous medium, and the content of Ag^+ in

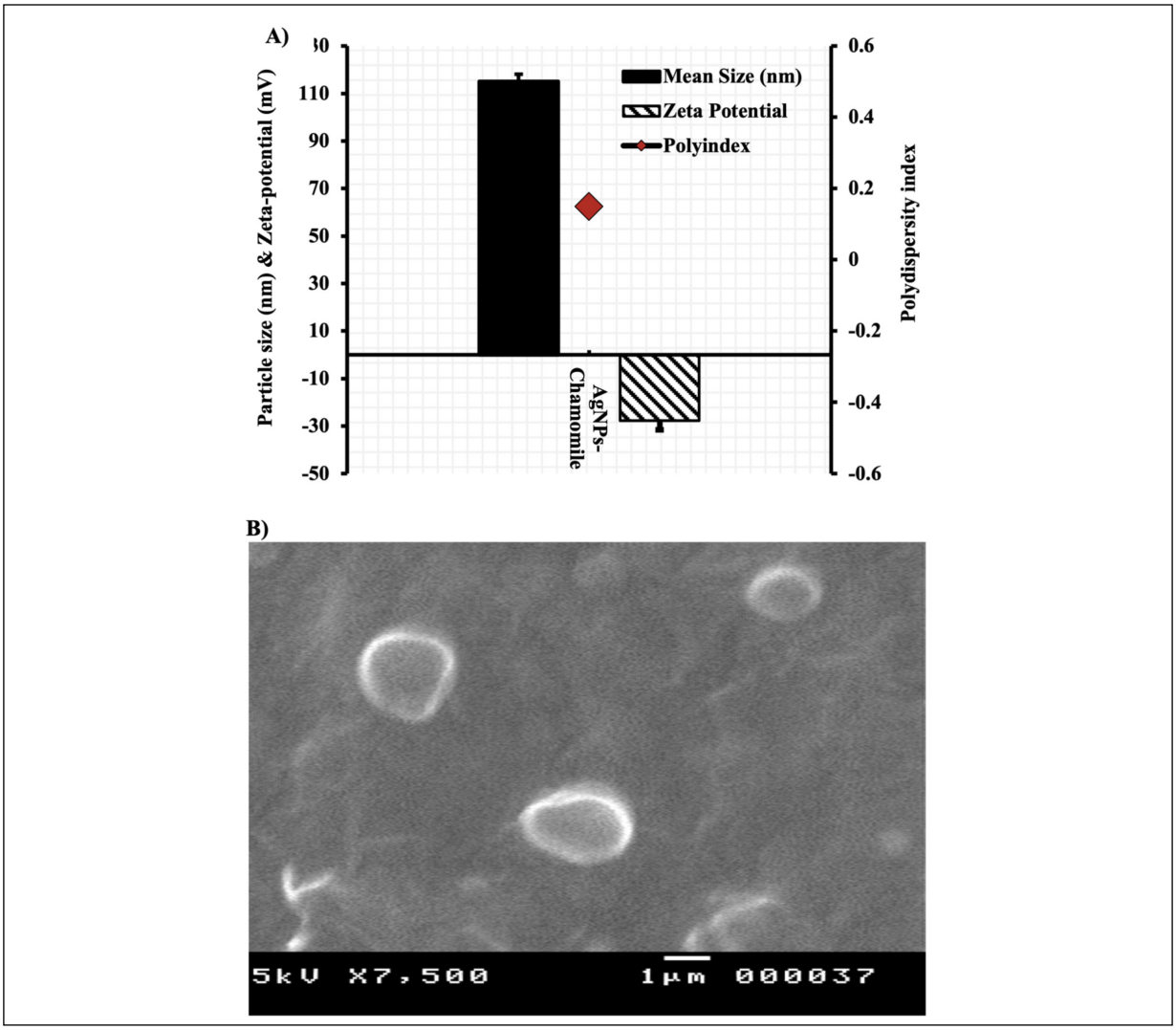

Figure 2. The diameter and ζ-potential of SNs-CHM as recorded by dynamic light scattering (**A**), SEM image of the formed SNs-CHM (**B**).

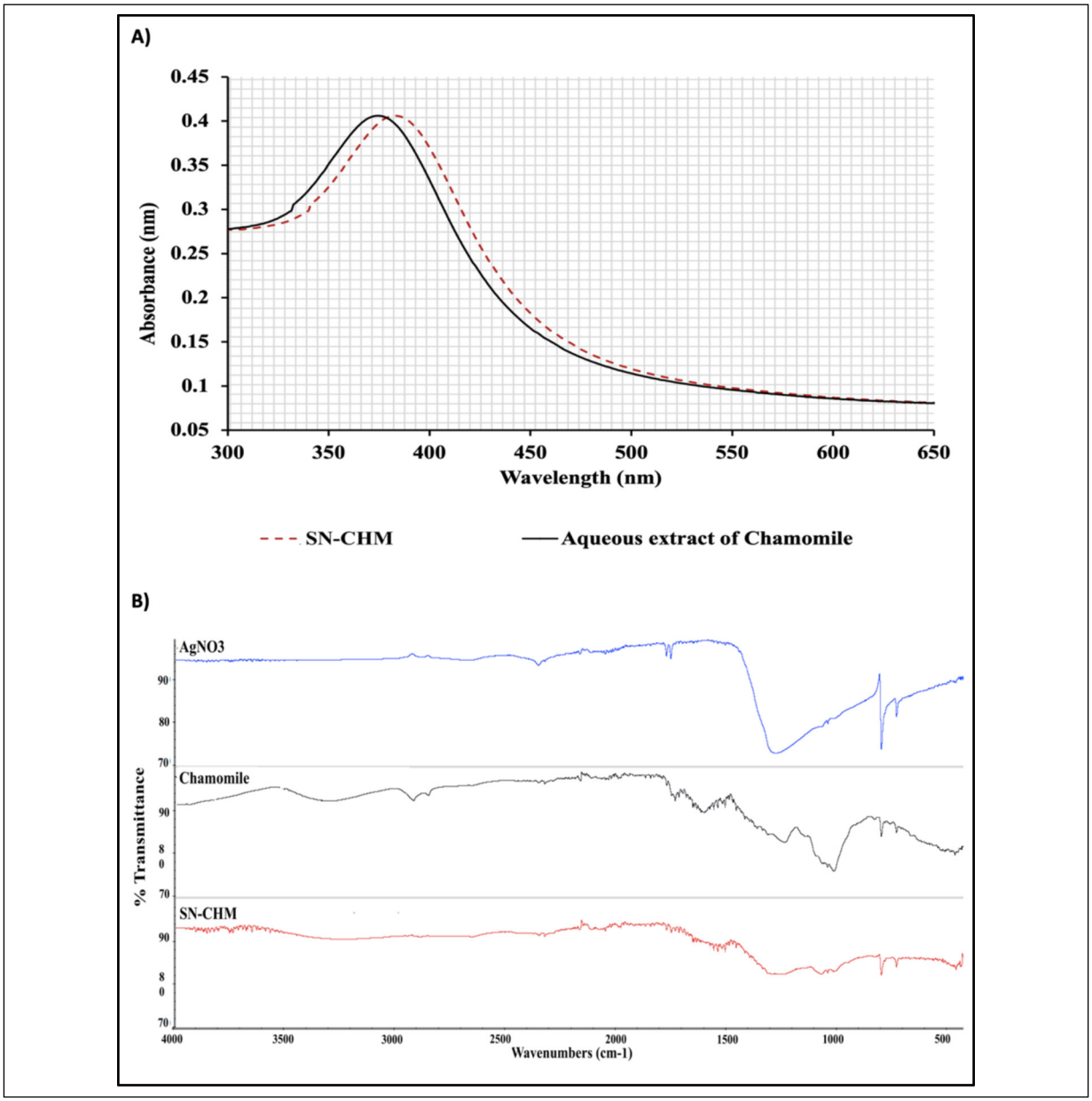

Figure 3. **A**, UV-spectroscopy of chamomile extract and SNs-CHM. **B**, FTIR spectra of silver nitrate compared with silver nanoparticles reduced by chamomile.

SN-CHM was completely released after 5 h. Ag^+ was released quickly from SN-CHM due to the higher solubility of CHM in water. Furthermore, a continual release of Ag^+ was observed depending on the degree of solubility of CHM in water (Figure 4A)[32]. The initial Ag^+ and Ag^0 concentrations contained in SN-CHM after NP synthesis were determined using ICP-OES. The yield percentage of Ag^0 in SN-CHM was 1.18 ± 29.1 mM (≈ 59.12%). The % yield does not reach 100% using the current process for synthesis with an acceptable % yield.

Antioxidant Activity of SN-CHM

Three methods were used to measure Chamomile extract antioxidant activity and whether its nanoparticle formulation with silver enhanced or decreased its activity with silver. The formulated Chamomile nanoparticles significantly reduced the molybdate ions compared to the Chamomile extract, with total antioxidant activity (TAA) values of 36.65 ± 0.88 and 31.33 ± 0.83, respectively. However, the reducing activity of the SN-CHM to the ferric ions in the FRAP was higher but not significant compared to the Chamomile extract

activity (FRAP values of 62.92 ± 0.84 and 61.77 ± 2.11). On the other hand, Chamomile extract was found to be more active as a free radical scavenger for DPPH (DPPH-SA) than SN-CHM, with DPPH-SA values of 12.50 ± 0.28 and 11.23 ± 0.82, respectively (Figure 4B).

Cell Proliferation Assay

Starting at 20 µg/mL, SN-CHM was proven to decrease the % viability of HT-29 cells at different concentrations (Figure 5A). Related results showed a metastatic colorectal cancer cell line of metastatic origin, SW620 cells, with extracts of CHM, $AgNO_3$, and SN-CHM resulted in significant dose inhibition of % viability starting at 10 µg/mL (Figure 5B). These findings thus demonstrate that the SN-CHM complex has anticancer potential in both adenocarcinoma and metastatic human colorectal cancer cell lines[33,34].

Gene Expression of Apoptosis-Related Genes

Based on the concentration of $AgNO_3$, SN-CHM, and CHM extracts were applied to HT-29

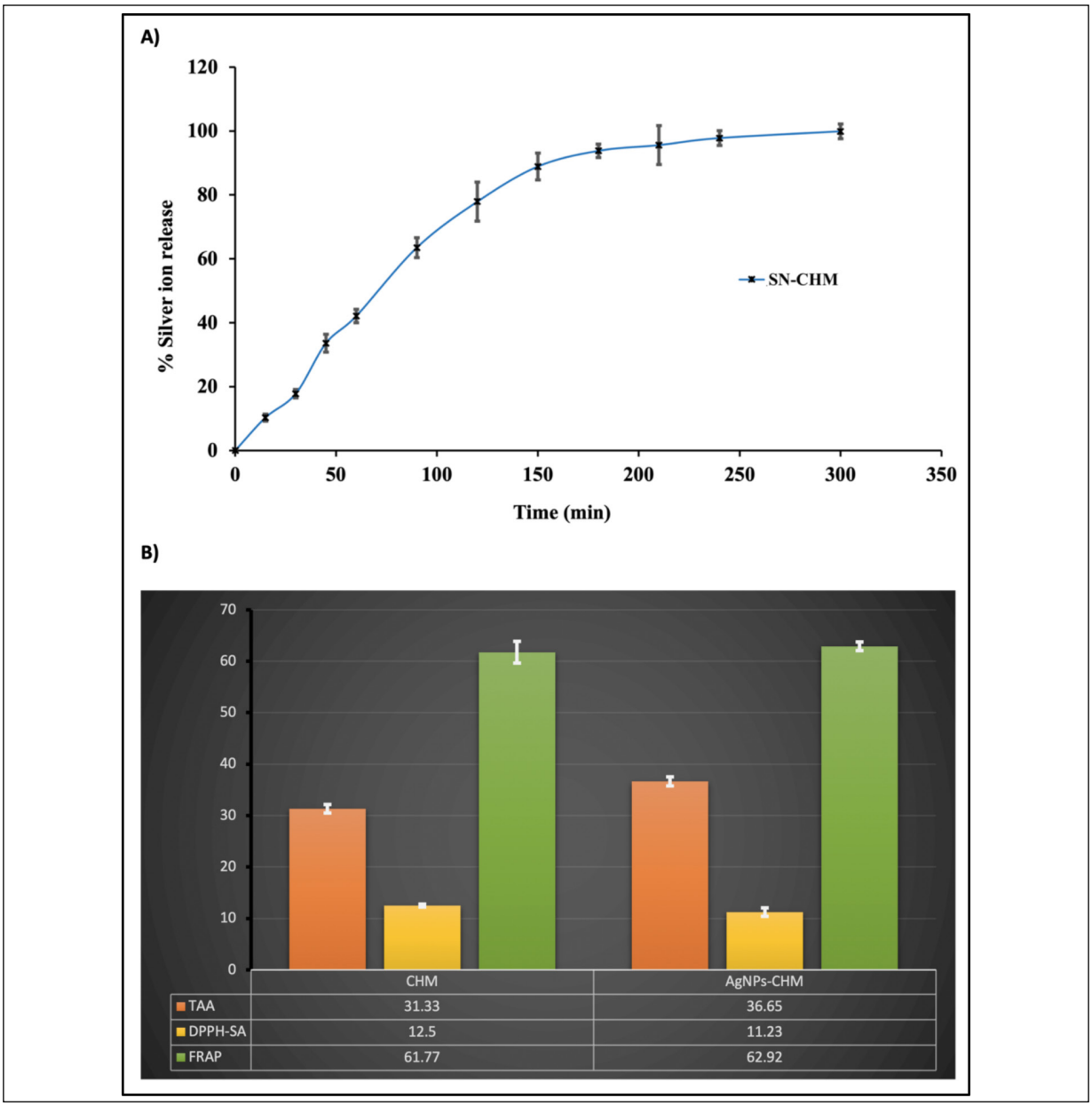

Figure 4. A, Ag^+ release from the prepared SNs-CHM in deionized water. (n = 3 ± S.D). **B**, Antioxidant activity of CHM and SNs-CHM using different TAA, DPPH-SA, and FRAP methods.

and SW620 cells for 48 h. The apoptosis and anti-apoptosis marker genes quantified by quantitative real-time PCR showed that SN-CAM can downregulate the anti-apoptotic genes BCL2 and BCL-Xl while significantly increasing the apoptotic gene BAX. The expression of *GAPDH*, a housekeeping gene, served as the standard to which all genes were normalized (Figure 6)[35].

Discussion

The aqueous extracts of the CHM were used to reduce $AgNO_3$, showing a color change from yellow to wine-red. This color change indicated the formed nanosilver SN-CHM (Figure 1). This change was due to the excitation of surface plasmon resonance by SNs, as revealed in the UV-Vis spectrum. The color change of the aqueous ethanolic extract to the synthesized SN-CHM confirmed the successful reduction with SN[9,32]. As reported, CHM-coated SNs (SNs-CHM) were synthesized[36]. SNs-CHM are more frequently synthesized chemically, where silver ions are decreased in the tested conditions[37], which may reduce the nucleation of the decreased (neutral) silver atoms. The use of small silver ion concentrations (mM range) increases the chance of nuclei formation. The stirring of the solution is to avoid the collision and develop-

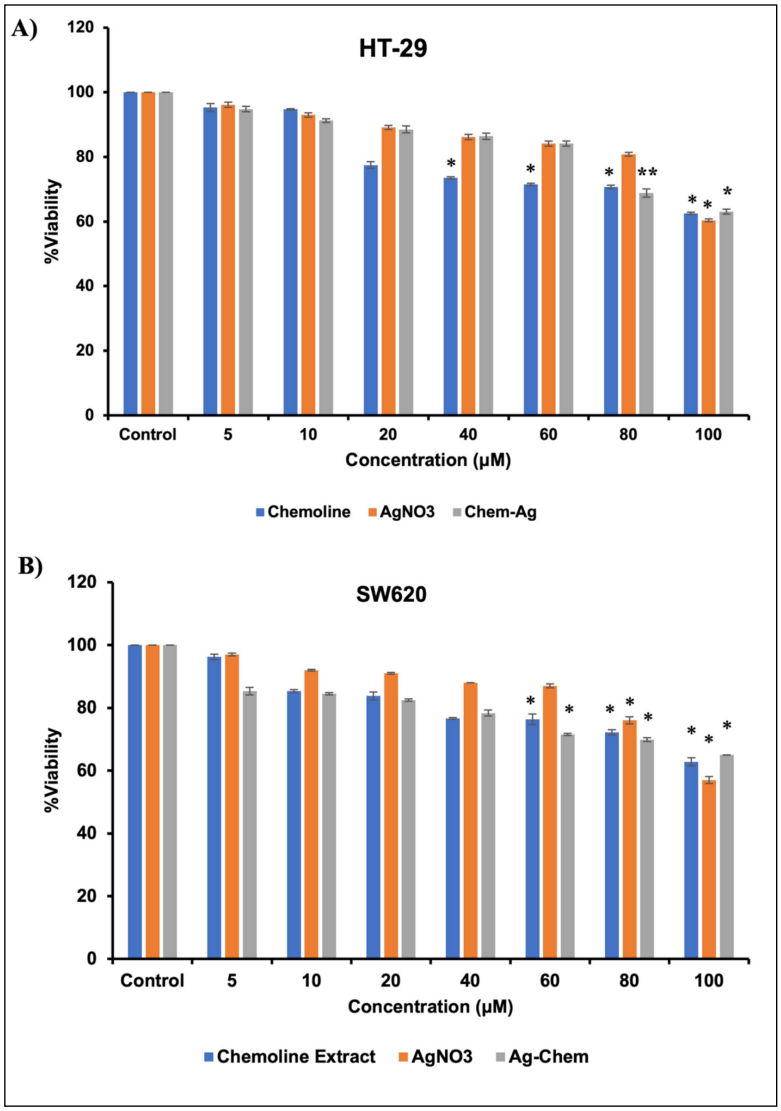

Figure 5. SNs-CHM inhibits cell proliferation. HT-29 (**A**) and SW620 (**B**) cells were treated with different concentrations of CHM, $AgNO_3$, and SNs-CHM. The results are expressed as the mean % viability of three independent determinations (*$p < 0.05$, **$p < 0.01$).

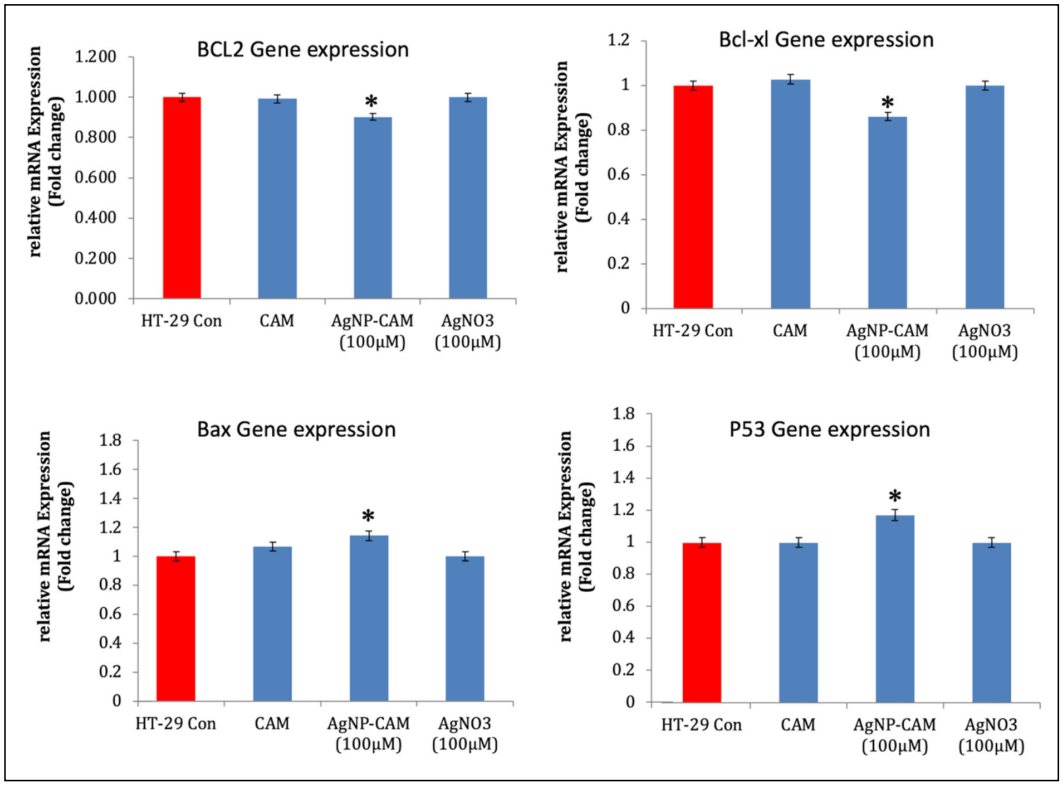

Figure 6. Quantitative real-time PCR gene expression analysis of proapoptotic and antiapoptotic genes in HT-29 cells treated with CHM and SNs-CHM. The results are the mean ± SD: *$p < 0.05$, **$p < 0.01$.

ment of silver nuclei. CHM is adsorbed on SN surfaces. The particles are "negatively loaded," and certain nanoparticles may be repelled[38].

CHM can inhibit the growth of cancer cells[39]; however, the formulated SNs-CHM have more powerful anticancer activity. Several flavonoids have been identified in the aqueous extract of Chamomile. For example, apigenin and apigenin-7-O-glucoside have been identified as major constituents in the High Performance Liquid Chromatography (HPLC) chromatogram of the flowers' aqueous extract[12]. In addition, several flavonoid aglycones and glycosides, e.g., apigenin 7-O-neohespridoside and apiin, luteolin-7-O-glucoside, myricitrin, hispidulin glucuronide, and luteolin-7-O-rutinoside, in addition to phenolic acids, e.g., p-coumaric acid, ferulic acid, caffeic acid, and chlorogenic acid, have been reported in the polar extracts of the plant[7,40]. These flavonoids and phenolic acids are supposed to be extracted by organic solvents and water and have been reported for their potential antioxidant and reducing activity[41]; therefore, they are expected to reduce the silver ions Ag^+ in the current study.

The % yield does not reach 100% using the current process for synthesis with an acceptable % yield. The decrease in % yield was due to the purification process, which resulted in the loss of SN-CHM. The adsorption of Ag^+ or SN-CHM on centrifuge tubes or pipets, volume loss, and transportation during sample dilution and quantification are possible causes of variations between actual and predicted Ag inputs[18]. UV-Vis spectroscopy is a critical technique for detecting colloidal silver. All metal nanoparticles have free electrons, so the SPR band shifts[30]. The surface plasmon resonance peak in the UV-VIS spectra of SN-CHM displayed a redshift, which is explained by the larger size of SN-CHM[30].

The increase in particle sizes reflected a change in color. Fuku et al[42], found that plasmonic NPs can be altered by changing the SPR absorption wavelength. The highly negatively charged ζ-potential of SN-CHM reveals that SN-CHM has enough charge to resist aggregation, confirming that SN-CHM is stable in a colloidal solution[43]. Moraes et al[44], reported that the size, polydispersity index (PDI), and ζ-potential of particles indicate the stability of NPs. Kaufman et al[45] stated that the surface charge of NPa plays a significant role in the stability of NPs.

PDI below 0.2 indicates homogeneous particle size distribution. PDIs lower than 0.2 are reported

to be ideal because they reveal that the particle size distribution falls within a narrow range of sizes[46]. The size of SN-CHM is different in DLS compared with that obtained by SEM due to the electronic images showing only the metallic center of the SN-CHM. The SEM captures only the core of the NPs, while the surrounding hydrated area CHM is considered the collapsed zone around Ag^0. The image procurement processes also showed a high-vacuum chamber[47]. Our interpretation agrees with the results due to the CHM coating of the SN-CHM, which limits the total particle density[48]. FTIR spectroscopy confirmed that a forming coat of CHM covers Ag^0 as SN-CHM to prevent the aggregation of SN. The FTIR showed the typical peaks of CHM and Ag compared with SN-CHM[49].

Furthermore, a continual release of Ag^+ was observed depending on the degree of solubility of CHM in water. Another study[50] showed that ethylcellulose had prolonged dissolution to 48 h because it is practically water-insoluble[51]. The shielding function of the coating film reduces the nanoparticle-water interaction, and therefore, particle corrosion is first limited by coating diffusion to water, slowing cation release. ICP-OES measurements proved the water solubility of SN-CHM, which confirmed that the depletion of CHM around SN increases the release rate of Ag^{+}[23].

The antioxidant assays revealed that SN-CHM enhanced the reducing ability of the Chamomile extract and had a nonsignificant effect on the free radical scavenging capacity of Chamomile. Similar effects for silver nanoparticles have been reported when they were used in the formulation of *Allium cepa* aqueous extract, as silver significantly enhanced the molybdenum ion-reducing power of the extract[52]. The viability assay showed in both cell lines that even CHM alone strongly reduced the viability of cancer cells. However, the strongest effect was seen on SN-CHM, which was significant, and this effect was best in HT-29 cells, with an approximately 40% reduction in cell viability. Cells treated with SN-CHM demonstrated a clear pattern in gene expression with the downregulation of anti-apoptotic markers and upregulation of pro-apoptotic marker genes, indicating that the CHM molecule has a pro-apoptotic effect in cancer cells.

SN-CHM can be useful as an anticancer drug since it targets the BCL2 family of proteins. Apoptosis is largely responsible for inhibiting cell growth and is a key factor in the fight against cancer[53]. As a result, apoptosis has become a popular therapeutic target for cancer treatment strategies. HT-29 and SW620 cells were significantly more susceptible to apoptosis when exposed to SN-CHM than control and CHM extract alone in this investigation. The most well-known method of killing cancer cells is the induction of apoptosis by anticancer treatment. SN-CHM was shown to be very efficient in inducing apoptosis by targeting BCL2, and it has the potential to be used as an anticancer therapy in the future.

Furthermore, the increased mortality of cells treated with SN-CHM is predicted due to the synergistic impact induced by reducing the CHM to Ago[54-56]. Following the findings of a recent study[57], employing the smallest possible nanoparticles may not be the best choice. The larger particles displayed greater resilience to external impacts than the smaller nanoparticles (NPs). The SN-CHM size can significantly influence in vitro toxicity compared with samples of a greater particle size retaining more activity against mammalian cells than those with a smaller particle size.

Furthermore, the size and form of nanoparticles have been shown to impact biological activity[58,59]. According to this study's findings, SN can be a very successful cancer therapy for many malignancies and an alternative treatment for inflammation prevention by promoting autophagy in the body[60]. Moreover, we prepared a simpler and more economical method of SN-CHM than that of Dadashpour et al[5], who prepared SNs-CHM by boiling the aqueous extract. We report here the difference that we did not use to boiling. The mix of CHM and $AgNO_3$ was mixed overnight, and the formulated SNs-CHM were prepared without boiling. Moreover, we used a lower concentration than Dadashpour et al[5], who used 60 μg/mL as a safer concentration of Ag^0. Moreover, the SN-CHM complex was found to inhibit the % viability of HT-29 and SW620 cells at different concentrations starting at 20 and 10 μg/mL, respectively, compared with extracts of CHM, $AgNO_3$, and SN-CHM.

Conclusions

When CHM is combined with Ag ions as anticancer nanoparticles, it has the potential to be a safe and effective soft drink with anticancer properties. Furthermore, SN-CHM is particularly effective in inhibiting the growth of

SW620 and HT-29 cell lines, suggesting that it could be a promising new treatment option for certain types of cancer. These findings are exciting and offer hope for those who are looking for safe and effective ways to fight cancer. In addition, this molecule has strong proapoptotic properties in cancer cell lines. SNs-CHM are promising NPs for future application in different fields and are very useful in developing antioxidant agents. At the same time, there is a need for further investigation in the future.

Acknowledgments
The authors extend their appreciation to the Deputyship for Research and Innovation, Ministry of Education, Saudi Arabia for funding this research. The authors also thank Qassim University for technical support.

Funding
This study was funded by the Deputyship for Research and Innovation, Ministry of Education, Saudi Arabia, through project number QU-IF-1-2-1.

ORCID ID
Ahmed A. H. Abdellatif: 0000-0002-3186-1896.

Conflict of Interest
All authors declare that they have no conflicts of interest.

Ethics Approval
Not applicable.

Informed Consent
Not applicable.

Data Availability
No data was used for the research described in the article.

Authors' Contributions
Conceptualization, Ahmed A. H. Abdellatif; Data curation, Ahmed A. H. Abdellatif and Hamdoon Mohammed; Formal analysis, Ahmed A. H. Abdellatif, Hamdoon Mohammed, Waad A. Samman and Aisha A. Alhaddad; Funding acquisition, Ahmed A. H. Abdellatif, Waad A. Samman, Osama Alrugaie and Mansour Alsharidah; Investigation, Ahmed A. H. Abdellatif, Maha-Hamadien Abdulla, Amer Mahmood and Noura Al Hassan; Methodology, Ahmed A. H. Abdellatif, Hamdoon Mohammed, Maha-Hamadien Abdulla, Amer Mahmood, Mansoor-Ali Vaali-Mohammed and Mansour Alsharidah; Project administration, Ahmed A. H. Abdellatif; Resources, Ahmed A. H. Abdellatif, Amal Al-Subaiyel, Aisha A. Alhaddad and Mansoor-Ali Vaali-Mohammed; Software, Ahmed A. H. Abdellatif and Waad A. Samman; Supervision, Ahmed A. H. Abdellatif and Mansour Alsharidah; Validation, Ahmed A. H. Abdellatif, Maha-Hamadien Abdulla, Amal Al-Subaiyel, Osama Alrugaie, Mansoor-Ali Vaali-Mohammed and Mansour Alsharidah; Visualization, Ahmed A. H. Abdellatif; Writing – original draft, Ahmed A. H. Abdellatif, Hamdoon Mohammed, Maha-Hamadien Hesham H. Taha, Abdulla, Waad A. Samman, Aisha A. Alhaddad, Osama Alrugaie, Mansoor-Ali Vaali-Mohammed, Noura Al Hassan and Mansour Alsharidah; Writing – review and editing, Ahmed A. H. Abdellatif, Hamdoon Mohammed, Maha-Hamadien Abdulla, Amer Mahmood, Aisha A. Alhaddad Hesham H. Taha, and Mansoor-Ali Vaali-Mohammed.

References

1) Luu TLA, Cao XT, Nguyen VT, Pham NL, Nguyen HL, Nguyen CT. Simple Controlling Ecofriendly Synthesis of Silver Nanoparticles at Room Temperature Using Lemon Juice Extract and Commercial Rice Vinegar. J Nanotechnol 2020; 2020: 1-9.
2) Ali ZA, Yahya R, Sekaran SD, Puteh R. Green Synthesis of Silver Nanoparticles Using Apple Extract and Its Antibacterial Properties. Adv Mater Sci Eng 2016; 2016: 1-6.
3) Bagherzade G, Tavakoli MM, Namaei MH. Green synthesis of silver nanoparticles using aqueous extract of saffron (Crocus sativus L.) wastages and its antibacterial activity against six bacteria. Asian Pac J Trop Biomed 2017; 7: 227-233.
4) Alshehri AA, Malik MA. Phytomediated Photo-Induced Green Synthesis of Silver Nanoparticles Using Matricaria chamomilla L. and Its Catalytic Activity against Rhodamine B. Biomolecules 2020; 10: 1604.
5) Dadashpour M, Firouzi-Amandi A, Pourhassan-Moghaddam M, Maleki MJ, Soozangar N, Jeddi F, Nouri M, Zarghami N, Pilehvar-Soltanahmadi Y. Biomimetic synthesis of silver nanoparticles using Matricaria chamomilla extract and their potential anticancer activity against human lung cancer cells. Mater Sci Eng C Mater Biol Appl 2018; 92: 902-912.
6) Al-Dabbagh B, Elhaty IA, Elhaw M, Murali C, Al Mansoori A, Awad B, Amin A. Antioxidant and anticancer activities of chamomile (Matricaria recutita L.). BMC Res Notes 2019; 12: 3.
7) Srivastava JK, Gupta S. Antiproliferative and apoptotic effects of chamomile extract in various human cancer cells. J Agric Food Chem 2007; 55: 9470-9478.
8) Wang X, Lin Y. Tumor necrosis factor and cancer, buddies or foes? Acta Pharmacol Sin 2008; 29: 1275-1288.

9) Abdellatif AAH, Rasheed Z, Alhowail AH, Alqasoumi A, Alsharidah M, Khan RA, Aljohani ASM, Aldubayan MA, Faisal W. Silver Citrate Nanoparticles Inhibit PMA-Induced TNFalpha Expression via Deactivation of NF-kappaB Activity in Human Cancer Cell-Lines, MCF-7. Int J Nanomedicine 2020; 15: 8479-8493.

10) Parlinska-Wojtan M, Kus-Liskiewicz M, Depciuch J, Sadik O. Green synthesis and antibacterial effects of aqueous colloidal solutions of silver nanoparticles using camomile terpenoids as a combined reducing and capping agent. Bioprocess Biosyst Eng 2016; 39: 1213-1223.

11) Srivastava JK, Shankar E, Gupta S. Chamomile: A herbal medicine of the past with bright future. Mol Med Rep 2010; 3: 895-901.

12) Srivastava JK, Gupta S. Extraction, Characterization, Stability and Biological Activity of Flavonoids Isolated from Chamomile Flowers. Mol Cell Pharmacol 2009; 1: 138.

13) Al-Sheddi ES, Farshori NN, Al-Oqail MM, Al-Massarani SM, Saquib Q, Wahab R, Musarrat J, Al-Khedhairy AA, Siddiqui MA. Anticancer Potential of Green Synthesized Silver Nanoparticles Using Extract of Nepeta deflersiana against Human Cervical Cancer Cells (HeLA). Bioinorg Chem Appl 2018; 2018: 9390784.

14) Kalishwaralal K, Deepak V, Ram Kumar Pandian S, Kottaisamy M, BarathmaniKanth S, Kartikeyan B, Gurunathan S. Biosynthesis of silver and gold nanoparticles using Brevibacterium casei. Colloids Surf B Biointerfaces 2010; 77: 257-262.

15) Mitra J, Shrivastava SL, Rao PS. Onion dehydration: a review. J Food Sci Technol 2012; 49: 267-277.

16) Gomaa EZ. Antimicrobial, antioxidant and antitumor activities of silver nanoparticles synthesized by Allium cepa extract: A green approach. J Genet Eng Biotechnol 2017; 15: 49-57.

17) Abdellatif AAH, Alhumaydhi FA, Al Rugaie O, Tolba NS, Mousa AM. Topical silver nanoparticles reduced with ethylcellulose enhance skin wound healing. Eur Rev Med Pharmacol Sci 2023; 27: 744-754.

18) Rahman A, Kumar S, Bafana A, Dahoumane SA, Jeffryes C. Biosynthetic Conversion of Ag(+) to highly Stable Ag(0) Nanoparticles by Wild Type and Cell Wall Deficient Strains of Chlamydomonas reinhardtii. Molecules 2018; 24: 98.

19) Abdellatif AAH. A plausible way for excretion of metal nanoparticles via active targeting. Drug Dev Ind Pharm 2020; 46: 744-750.

20) Patel N, Lalwani D, Gollmer S, Injeti E, Sari Y, Nesamony J. Development and evaluation of a calcium alginate based oral ceftriaxone sodium formulation. Prog Biomater 2016; 5: 117-133.

21) Abdellatif AAH, Ibrahim MA, Amin MA, Maswadeh H, Alwehaibi MN, Al-Harbi SN, Alharbi ZA, Mohammed HA, Mehany ABM, Saleem I. Cetuximab Conjugated with Octreotide and Entrapped Calcium Alginate-beads for Targeting Somatostatin Receptors. Sci Rep 2020; 10: 4736.

22) Abdellatif AAH, Alawadh SH, Bouazzaoui A, Alhowail AH, Mohammed HA. Anthocyanins rich pomegranate cream as a topical formulation with anti-aging activity. J Dermatolog Treat 2021; 32: 983-990.

23) Fortunati E, Latterini L, Rinaldi S, Kenny JM, Armentano I. PLGA/Ag nanocomposites: in vitro degradation study and silver ion release. J Mater Sci Mater Med 2011; 22: 2735-2744.

24) Aroua LM, Almuhaylan HR, Alminderej FM, Messaoudi S, Chigurupati S, Al-Mahmoud S, Mohammed HA. A facile approach synthesis of benzoylaryl benzimidazole as potential alpha-amylase and alpha-glucosidase inhibitor with antioxidant activity. Bioorg Chem 2021; 114: 105073.

25) Mohammed HA. Phytochemical Analysis, Antioxidant Potential, and Cytotoxicity Evaluation of Traditionally Used Artemisia absinthium L. (Wormwood) Growing in the Central Region of Saudi Arabia. Plants (Basel) 2022; 11: 1028.

26) Aroua LM, Alosaimi AH, Alminderej FM, Messaoudi S, Mohammed HA, Almahmoud SA, Chigurupati S, Albadri AEAE, Mekni NH. Synthesis, Molecular Docking, and Bioactivity Study of Novel Hybrid Benzimidazole Urea Derivatives: A Promising α-Amylase and α-Glucosidase Inhibitor Candidate with Antioxidant Activity. Pharmaceutics 2023; 15: 457.

27) Mohammed HA, Al-Omar MS, Mohammed SAA, Aly MSA, Alsuqub ANA, Khan RA. Drying Induced Impact on Composition and Oil Quality of Rosemary Herb, Rosmarinus Officinalis Linn. Molecules 2020; 25: 2830.

28) Abdellatif AAH, Abdelfattah A, Bouazzaoui A, Osman SK, Al-Moraya IS, Showail AMS, Alsharidah M, Aboelela A, Al Rugaie O, Faris TM, Tawfeek HM. Silver Nanoparticles Stabilized by Poly (Vinyl Pyrrolidone) with Potential Anticancer Activity towards Prostate Cancer. Bioinorg Chem Appl 2022; 2022: 6181448.

29) Abdellatif AAH, Alsharidah M, Al Rugaie O, Tawfeek HM, Tolba NS. Silver Nanoparticle-Coated Ethyl Cellulose Inhibits Tumor Necrosis Factor-alpha of Breast Cancer Cells. Drug Des Devel Ther 2021; 15: 2035-2046.

30) Ranoszek-Soliwoda K, Tomaszewska E, Socha E, Krzyczmonik P, Ignaczak A, Orlowski P, Krzyzowska M, Celichowski G, Grobelny J. The role of tannic acid and sodium citrate in the synthesis of silver nanoparticles. J Nanopart Res 2017; 19: 273.

31) Nabikhan A, Kandasamy K, Raj A, Alikunhi NM. Synthesis of antimicrobial silver nanoparticles by callus and leaf extracts from saltmarsh plant, Sesuvium portulacastrum L. Colloids Surf B Biointerfaces 2010; 79: 488-493.

32) Abdellatif AAH, Alturki HNH, Tawfeek HM. Different cellulosic polymers for synthesizing silver nanoparticles with antioxidant and antibacterial activities. Sci Rep 2021; 11: 84.

33) Abdellatif AA, Zayed G, El-Bakry A, Zaky A, Saleem IY, Tawfeek HM. Novel gold nanoparticles coated with somatostatin as a potential delivery system for targeting somatostatin receptors. Drug Dev Ind Pharm 2016; 42: 1782-1791.

34) Abdellatif AAH, Alhathloul SS, Aljohani ASM, Maswadeh H, Abdallah EM, Hamid Musa K, El Hamd MA. Green Synthesis of Silver Nanoparticles Incorporated Aromatherapies Utilized for Their Antioxidant and Antimicrobial Activities against Some Clinical Bacterial Isolates. Bioinorg Chem Appl 2022; 2022: 2432758.

35) Abdellatif AAH, Tolba NS, Alsharidah M, Al Rugaie O, Bouazzaoui A, Saleem I, Maswadeh H, Ali AT. PEG-4000 formed polymeric nanoparticles loaded with cetuximab downregulate p21 & stathmin-1 gene expression in cancer cell lines. Life Sci 2022; 295: 120403.

36) Afshinnia K, Baalousha M. Effect of phosphate buffer on aggregation kinetics of citrate-coated silver nanoparticles induced by monovalent and divalent electrolytes. Sci Total Environ 2017; 581-582: 268-276.

37) Khan Z, Al-Thabaiti SA, Obaid AY, Al-Youbi AO. Preparation and characterization of silver nanoparticles by chemical reduction method. Colloids Surf B Biointerfaces 2011; 82: 513-517.

38) Bastús NG, Merkoçi F, Piella J, Puntes V. Synthesis of Highly Monodisperse Citrate-Stabilized Silver Nanoparticles of up to 200 nm: Kinetic Control and Catalytic Properties. Chem Mater 2014; 26: 2836-2846.

39) Kato A, Minoshima Y, Yamamoto J, Adachi I, Watson AA, Nash RJ. Protective effects of dietary chamomile tea on diabetic complications. J Agric Food Chem 2008; 56: 8206-8211.

40) Sotiropoulou NS, Megremi SF, Tarantilis P. Evaluation of Antioxidant Activity, Toxicity, and Phenolic Profile of Aqueous Extracts of Chamomile (Matricaria chamomilla L.) and Sage (Salvia officinalis L.) Prepared at Different Temperatures. Applied Sciences 2020; 10: 2270.

41) Mohammed HA, Al-Omar MS, Khan RA, Mohammed SAA, Qureshi KA, Abbas MM, Al Rugaie O, Abd-Elmoniem E, Ahmad AM, Kandil YI. Chemical Profile, Antioxidant, Antimicrobial, and Anticancer Activities of the Water-Ethanol Extract of Pulicaria undulata Growing in the Oasis of Central Saudi Arabian Desert. Plants (Basel) 2021; 10: 1811.

42) Fuku K, Hayashi R, Takakura S, Kamegawa T, Mori K, Yamashita H. The synthesis of size- and color-controlled silver nanoparticles by using microwave heating and their enhanced catalytic activity by localized surface plasmon resonance. Angew Chem Int Ed Engl 2013; 52: 7446-7450.

43) Greenwood R, Kendall K. Selection of suitable dispersants for aqueous suspensions of zirconia and titania powders using acoustophoresis. J Eur Ceram Soc 1999; 19: 479-488.

44) Moraes CM, De Paula E, Rosa AH, Fraceto LF. Physicochemical Stability of Poly(lactide-co-glycolide) Nanocapsules Containing the Local Anesthetic Bupivacaine. J Braz Chem Soc 2010; 21: 995-1000.

45) Kaufman ED, Belyea J, Johnson MC, Nicholson ZM, Ricks JL, Shah PK, Bayless M, Pettersson T, Feldoto Z, Blomberg E, Claesson P, Franzen S. Probing protein adsorption onto mercaptoundecanoic acid stabilized gold nanoparticles and surfaces by quartz crystal microbalance and zeta-potential measurements. Langmuir 2007; 23: 6053-6062.

46) Vieville J, Tanty M, Delsuc MA. Polydispersity index of polymers revealed by DOSY NMR. J Magn Reson 2011; 212: 169-73.

47) Fissan H, Ristig S, Kaminski H, Asbach C, Epple M. Comparison of different characterization methods for nanoparticle dispersions before and after aerosolization. Analytical Methods 2014; 6: 7324-7334.

48) Zheng T, Bott S, Huo Q. Techniques for Accurate Sizing of Gold Nanoparticles Using Dynamic Light Scattering with Particular Application to Chemical and Biological Sensing Based on Aggregate Formation. ACS Appl Mater Interfaces 2016; 8: 21585-21594.

49) Sunkar S, Nachiyar CV. Biogenesis of antibacterial silver nanoparticles using the endophytic bacterium Bacillus cereus isolated from Garcinia xanthochymus. Asian Pac J Trop Biomed 2012; 2: 953-959.

50) Duarte AR, Gordillo MD, Cardoso MM, Simplicio AL, Duarte CM. Preparation of ethyl cellulose/methyl cellulose blends by supercritical antisolvent precipitation. Int J Pharm 2006; 311: 50-54.

51) Raut NS, Somvanshi S, Jumde AB, Khandelwal HM, Umekar MJ, Kotagale NR. Ethyl cellulose and hydroxypropyl methyl cellulose buoyant microspheres of metoprolol succinate: Influence of pH modifiers. Int J Pharm Investig 2013; 3: 163-170.

52) Abdellatif AAH, Mahmood A, Alsharidah M, Mohammed HA, Alenize SK, Bouazzaoui A, Al Rugaie O, Alnuqaydan AM, Ahmad R, Vaali-Mohammad M-A, Alfayez M, Traiki TB, Al-Regaiey KA, Ali AT, Hassan YAH, Abdulla MH, Liu J. Bioactivities of the Green Synthesized Silver Nanoparticles Reduced Using Allium cepa L Aqueous Extracts Induced Apoptosis in Colorectal Cancer Cell Lines. J Nanomater 2022; 2022: 1-13.

53) Carneiro BA, El-Deiry WS. Targeting apoptosis in cancer therapy. Nat Rev Clin Oncol 2020; 17: 395-417.

54) Ghosal K, Ghosh S, Ghosh D, Sarkar K. Natural polysaccharide derived carbon dot based in situ facile green synthesis of silver nanoparticles: Synergistic effect on breast cancer. Int J Biol Macromol 2020; 162: 1605-1615.

55) R N, S M, S JP, P P. Green synthesis and characterization of bioinspired silver, gold and platinum nanoparticles and evaluation of their synergistic antibacterial activity after combining with different classes of antibiotics. Mater Sci Eng C Mater Biol Appl 2019; 96: 693-707.

56) Tippayawat P, Phromviyo N, Boueroy P, Chompoosor A. Green synthesis of silver nanoparticles in aloe vera plant extract prepared by a hydrothermal method and their synergistic antibacterial activity. PeerJ 2016; 4: e2589.

57) Belteky P, Ronavari A, Zakupszky D, Boka E, Igaz N, Szerencses B, Pfeiffer I, Vagvolgyi C, Kiric-

si M, Konya Z. Are Smaller Nanoparticles Always Better? Understanding the Biological Effect of Size-Dependent Silver Nanoparticle Aggregation Under Biorelevant Conditions. Int J Nanomedicine 2021; 16: 3021-3040.

58) Wang X, Cui X, Zhao Y, Chen C. Nano-bio interactions: the implication of size-dependent biological effects of nanomaterials. Sci China Life Sci 2020; 63: 1168-1182.

59) Busila M, Tabacaru A, Mussat V, Vasile BS, Neasu IA, Pinheiro T, Roma-Rodrigues C, Baptista PV, Fernandes AR, Matos AP, Marques F. Size-Dependent Biological Activities of Fluorescent Organosilane-Modified Zinc Oxide Nanoparticles. J Biomed Nanotechnol 2020; 16: 137-152.

60) Jabir MS, Saleh YM, Sulaiman GM, Yaseen NY, Sahib UI, Dewir YH, Alwahibi MS, Soliman DA. Green Synthesis of Silver Nanoparticles Using Annona muricata Extract as an Inducer of Apoptosis in Cancer Cells and Inhibitor for NLRP3 Inflammasome via Enhanced Autophagy. Nanomaterials (Basel) 2021; 11: 384.